Electromagnetic Tomography (EMT) Metal Flaw Detection System Based on Improved BP Neural Network

Chunguang Sun, He Min

School of Logistics Engineering, Shanghai Maritime University, Shanghai 201306, China.

945428524@qq.com

Abstract

In electromagnetic tomography (EMT), the image reconstruction equation is often ill-conditioned, and the prior information that can be obtained is also limited, resulting in low image reconstruction accuracy. In this paper, an improved BP neural network algorithm is used to fit the non-linear mapping relationship between the measurement data and the image gray matrix by learning enough representative sample data. Without the need for a sensitivity matrix, the conversion from measurement data to image reconstruction is realized. Respectively use the linear back projection algorithm (LBP), the traditional BP neural network algorithm and the LM (Levenberg-Marquardt)-BP neural network algorithm to reconstruct the image of the simulated data, and find the accuracy and clarity of the image reconstruction of the LM-BP neural network algorithm Significantly improved. In the experiment, a 6-coil electromagnetic tomography system with STM32 as the controller was built. After actual measurement data, different algorithms were used for image reconstruction, which verified the conclusion of the simulation experiment and provided a feasible scheme for electromagnetic tomography.

Keywords

Electromagnetic tomography; BP neural network; Image reconstruction; 6 coils.

1. Introduction

The use of metal materials can be seen everywhere in life, so the detection of metal materials is becoming more and more common. In addition to regular manual inspections, automatic detection of crack defects is also required during the production, processing, and use of metal materials. With the continuous improvement of production automation, there is an urgent need for efficient and accurate nondestructive testing technology. Commonly used non-destructive testing methods include radiographic testing, magnetic particle testing, ultrasonic testing, etc[1], but when applied to metal fixed-point online testing, the effect is not ideal.

Electromagnetic tomography (EMT) technology is based on the principle of electromagnetic induction and has the advantages of non-contact, fast speed, low cost, and online detection[2]. EMT achieves the purpose of detecting the distribution of the object by detecting the electrical conductivity distribution of the measured object. It has been used in many fields, such as industrial multiphase flow detection, metal tomography, mineral exploration, etc. The main goal of EMT technology is to reconstruct the image of the measured object[3, 4]. Commonly used image reconstruction algorithms are mainly divided into iterative algorithms and non-iterative algorithms. Iterative algorithms include Landweber iterative algorithm, conjugate gradient (CG algorithm), non-iterative algorithms include linear back projection (LBP) algorithm, Tikhonov regularization algorithm, truncated singular value decomposition (TSVD) algorithm. Due to the non-linear relationship between the conductivity distribution and the voltage, it is difficult to achieve high-quality image reconstruction with non-iterative algorithms based on simple linear models. Therefore, although the linear back projection (LBP) algorithm has a fast reconstruction speed, the imaging quality is poor, and the resolution is not high, and other algorithms used for metal flaw detection in electromagnetic tomography also have certain limitations.

This article first analyzes the basic principles of electromagnetic tomography, uses the nonlinear human brain thinking of neural network[5], and uses the improved BP neural network algorithm (LM-BP neural network algorithm) to fit the detection data and the corresponding reconstructed image. Through simulation experiments, it is found that the image reconstruction effect of this method is better, and it has also been verified on the hardware experimental platform.

2. Introduction and image reconstruction of EMT metal flaw detection system

2.1 The basic principle of EMT metal flaw detection system

The EMT system consists of a controller, an excitation source, a sensor coil, a signal conditioning circuit, and a host computer. The overall structure diagram is shown in Fig. 1. The sensor coil is placed on the surface of the metal to be measured when used, and the excitation signal is input to the excitation coil in the sensor. Resulting in a changing magnetic field. According to the Faraday electromagnetic induction principle, it is known that eddy currents will be generated on the metal surface. Because the excitation signal is changed, the magnetic field generated by the eddy current is also changed. The defect of the measured metal surface will affect the eddy current generation. Magnetic field, the induced voltage on the detection coil within the magnetic field will also change, and the collected induced voltage can be obtained through a certain algorithm to obtain the conductivity distribution of the measured metal, thereby obtaining metal surface defect information.

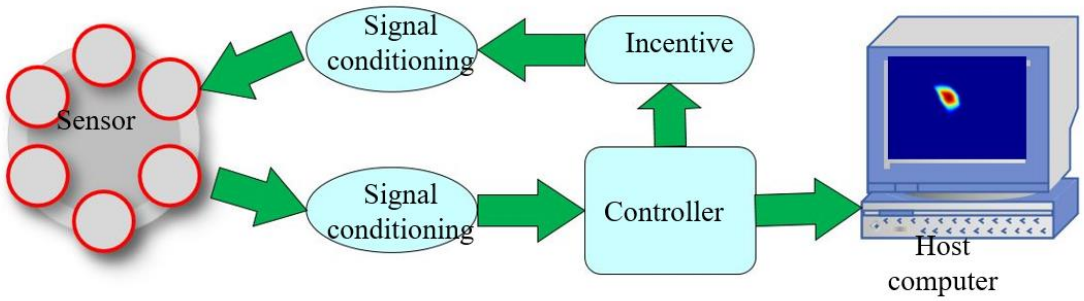

Fig. 1 T EMT metal flaw detection system structure diagram

2.2 Image reconstruction of EMT system

The image reconstruction of EMT belongs to solving the ill-posed inverse problem, and the mathematical model is shown in formula (1):

$$v = F(\sigma) \tag{1}$$

Where σ represents the conductivity distribution, v indicates the detection coil voltage, F is the nonlinear ill-posed function of the EMT system, Equation (1) can be expressed as Equation (2):

$$v = F(\sigma) = F(\sigma_0) + \frac{\partial F}{\partial \sigma}\Big|_{\sigma_0} (\sigma - \sigma_0) + o(\|\sigma - \sigma_0\|_2) \tag{2}$$

In the equation $\frac{\partial F}{\partial \sigma}$ representative sensitivity matrix, σ_0 indicates the electrical conductivity distribution without defects, Equation 2 can be simplified to Equation 3.

$$v - F(\sigma_0) = S(\sigma - \sigma_0) \tag{3}$$

$$B = SG \tag{4}$$

In the above formula $B = v - F(\sigma_0)$, indicates the amount of change in the voltage of the detection coil caused by the change in the conductivity or magnetic permeability of the measured metal,G represents the conductivity distribution matrix. The conventional method is to calculate the sensitivity matrix S based on prior information, Then use a certain algorithm according to the detected data B to get the conductivity distribution matrix G.

3. Introduction of BP neural network

3.1 Traditional BP neural network

BP (Back Propagation) neural network is a method of neural learning training. It belongs to supervised learning. BP network is composed of two processes of forward propagation of learning information and back propagation of error. It can learn and store a amounts of input-output mapping relationship can theoretically approximate any nonlinear continuous function, and the process of EMT image reconstruction is the process of nonlinear mapping. A neural network usually consists of an input layer, a hidden layer, and an output layer, as shown in Fig. 2. The input layer is used to receive external information, and after processing it is passed to the neurons in the hidden layer. The number of neurons in the input layer is equal to the number of features of each group of data. The hidden layer is responsible for internal information processing. According to the information change ability, the hidden layer can be a single layer or a multi-layer structure. Generally, a single layer is commonly used. The general principle for setting the number of neurons in the hidden layer is: correctly reflect the input On the basis of the relationship with the output, use fewer neurons to make the network structure as simple as possible. This article first sets a smaller number of interneurons, and continuously increases the number of interneurons. After learning and training, test the error situation, and finally determine the most suitable one. number. The output layer is used to output processing information to the outside world, and the number of neurons is related to the number of pixels in the region of interest. When the actual output is different from the expected output, the error is propagated back, the error passes through the output layer, and the weights of each layer are corrected in a way that the error gradient drops.

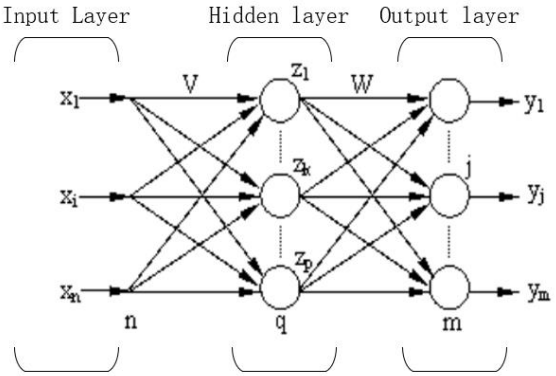

Fig. 2 Common neural network structure model

3.2 Improved BP neural network and its application

The input part of the neural network is the voltage data measured by the sensor, and the output part is the corresponding image gray matrix. Large amounts of representative data with object field characteristics are used for learning to determine the various parameters of the network and automatically learn the relationship between input and output. Relationship, there is no need to establish a sensitivity matrix. However, the classic BP algorithm is to perform forward operations on each sample data and continuously modify the weights, so that only each sample can be calculated separately. When dealing with complex problems, the convergence speed is slow and the accuracy is low[6], while LM(The Levenberg-Marquardt) algorithm uses all sample information to modify the weight matrix. This algorithm is derived from the classic Newton algorithm and uses the nonlinear

least square method to derive the approximate form of the Hessian matrix, which improves the convergence speed and accuracy, and has been successfully applied[7].

Assume that the BP neural network consists of M layers, Q pair of sample data (pq, yq), q=1, 2,…,Q. among them pq is columns vector of R elements, represents the q pair of sample input vectors. yq is SM-element column vector, represents the ideal output vector of the q pair of training samples. Let $\bar{y}_q$ be a column vector of SM elements, represents the actual output vector corresponding to the Q-th pair of samples. Suppose the number of neurons in the input layer is R, let the input layer be layer 0, The number of neurons in the m-th layer is Sm, m=1,2, …,M. The number of neurons in the output layer is SM. $e_q = y_q - \bar{y}_q$, let $w_{i,j}^m$ be the connection weight from the j-th neuron of the (m-1)-th layer to the i-th neuron of the mth layer, w^m is the $m(m \geq 1)$ layer weight matrix, bm is the offset column vector of the $m(m \geq 1)$-th layer, respectively as follows:

$$w = \begin{bmatrix} w_{1,1}^m & w_{1,2}^m & \cdots & w_{1,S^{m-1}}^m \\ w_{2,1}^m & w_{2,2}^m & \cdots & w_{2,S^{m-1}}^m \\ \vdots & \vdots & \ddots & \vdots \\ w_{S^m,1}^m & w_{S^m,2}^m & \cdots & w_{S^m,S^{m-1}}^m \end{bmatrix} \tag{5}$$

$$b^m = \left[b_1^m, b_2^m, ..., b_{S^m}^m \right]^T \tag{6}$$

The training purpose of the BP algorithm is to minimize the error sum of squares between the expected output and the actual output. This error sum of squares function is the objective function F that needs to be optimized:

$$F(x) = E(w) = \sum_{q=1}^{Q} (y_q - \bar{y}_q)^T (y_q - \bar{y}_q) = \sum_{q}^{Q} E_q(w)^T E_q(w) = \sum_{q=1}^{Q} \sum_{j=1}^{S^M} [E_{j,q}(w)]^2 \tag{7}$$

According to Newton's method[8]:

$$w(k+1) = w(k) - H_k^{-1} g_k \tag{8}$$

Among them: H_k is the Hessian matrix; g_k is the gradient. Has the following definition:

$$P = QS^M \tag{9}$$

The optimized objective function can be expressed as:

$$E(w) = \sum_{p=1}^{p} E_p^2(w) \tag{10}$$

The gradient of the objective function is:

$$g^m(w) = \Delta E^m(w) = \begin{bmatrix} \frac{\partial \sum_{p=1}^{p} E_p(w)^2}{\partial w^1} \\ \frac{\partial \sum_{p=1}^{p} E_p(w)^2}{\partial w^2} \\ \vdots \\ \frac{\partial \sum_{p=1}^{p} E_p(w)^2}{\partial w^{S^m}} \end{bmatrix} = 2 \begin{bmatrix} E_p(w) \frac{\partial \sum_{p=1}^{p} E_p(w)}{\partial w^1} \\ E_p(w) \frac{\partial \sum_{p=1}^{p} E_p(w)}{\partial w^2} \\ \vdots \\ E_p(w) \frac{\partial \sum_{p=1}^{p} E}{} \end{bmatrix} = 2 J^m(w)^T E_p(w) \tag{11}$$

So:

$$J^m(w) = [\frac{\partial E_p}{\partial w^1} \frac{\partial E_p}{\partial w^2} \cdots \frac{\partial E_p}{\partial w^{S^m}}] \tag{12}$$

And because:

$$E^T = \left[E_{1,1}, \cdots, E_{S^M,1}, E_{2,1}, \cdots, E_{S^M,2}, \cdots, E_{1,Q}, \cdots, E_{S^M,Q} \right] \tag{13}$$

The weight vector w is: $w^T = [w^1, w^2, \cdots, w^M]$

And because:

$$w^i = \left[w^i_{1,1}, w^i_{1,2}, \cdots, w^i_{1,S^{i-1}}, w^j_{2,1}, w^j_{2,2}, \cdots, w^i_{2,S^{i-1}}, \cdots, w_{S^i,S^{i-1}} \right] \tag{14}$$

Jacobian matrix:

$$J^m(w) = \begin{bmatrix} \frac{\partial E_{1,1}}{\partial w^1} & \frac{\partial E_{1,1}}{\partial w^2} & \cdots & \frac{\partial E_{1,1}}{\partial w^{S^m}} \\ \frac{\partial E_{2,1}}{\partial w^1} & \frac{\partial E_{2,1}}{\partial w^2} & \cdots & \frac{\partial E_{2,1}}{\partial w^{S^m}} \\ \vdots & \vdots & & \vdots \\ \frac{\partial E_{S^M,1}}{\partial w^1} & \frac{\partial E_{S^M,1}}{\partial w^2} & & \frac{\partial E_{S^M,1}}{\partial w^{S^m}} \\ \frac{\partial E_{1,2}}{\partial w^1} & \frac{\partial E_{1,2}}{\partial w^2} & & \frac{\partial E_{1,2}}{\partial w^{S^m}} \\ \frac{\partial E_{2,2}}{\partial w^1} & \frac{\partial E_{2,2}}{\partial w^2} & & \frac{\partial E_{2,2}}{\partial w^{S^m}} \\ \vdots & \vdots & & \vdots \\ \frac{\partial E_{S^M,2}}{\partial w^1} & \frac{\partial E_{S^M,2}}{\partial w^2} & & \frac{\partial E_{S^M,2}}{\partial w^{S^m}} \\ \vdots & \vdots & & \vdots \\ \frac{\partial E_{1,Q}}{\partial w^1} & \frac{\partial E_{1,Q}}{\partial w^2} & & \frac{\partial E_{1,Q}}{\partial w^{S^m}} \\ \frac{\partial E_{2,Q}}{\partial w^1} & \frac{\partial E_{2,Q}}{\partial w^2} & & \frac{\partial E_{2,Q}}{\partial w^{S^m}} \\ \vdots & \vdots & & \vdots \\ \frac{\partial E_{S^M,Q}}{\partial w^1} & \frac{\partial E_{S^M,Q}}{\partial w^2} & & \frac{\partial E_{S^M,Q}}{\partial w^{S^m}} \end{bmatrix} \tag{15}$$

Then find the Hessian matrix, where the k and j elements of the Hessian matrix are:

$$\left[\Delta^2 E(w)\right]_{k,j} = \frac{\partial^2 E(w)}{\partial w_k \partial w_j} = 2\sum_{p=1}^{p} (\frac{\partial E_p}{\partial w_k} \frac{\partial E_p}{\partial w_j} + E_p \frac{\partial^2 E_p}{\partial w_k \partial w_j}) \tag{16}$$

Thus the Hessian matrix can be expressed as: $\Delta^2 E(w) = 2J_k(w)^T J_k(w) + 2S$

Where matrix S is the second derivative matrix of $S^m \times S^m$:

$$S = \sum_{p=1}^{p} E_p \Delta^2 E_p(w) \tag{17}$$

When the objective function reaches the minimum, the elements of matrix S become very small and can be ignored. The Hessian matrix can be approximately expressed as:

$$H \approx 2J_k(w)^T J_k(w) \tag{18}$$

Substitute the Hessian matrix and gradient into Newton's formula:

$$w^m(K+1) = w^m(k) - \left[J_k^m(w)^T J_k^m(w) \right]^{-1} J_k^m(w)^T E_k^m(w) \tag{19}$$

However, there will also be problems in the above iterations. $H = J_k{}^T J_k$ may be a singular matrix and needs further correction:

$$H \approx J_k{}^T J_k + u_k I \tag{20}$$

u_k is the learning rate, I is the unit matrix, the Levenberg-Marquardt algorithm for updating network weights is obtained, referred to as the LM-BP algorithm:

$$w(k+1) = w(k) - \left[J_k{}^T J_k + u_k I \right]^{-1} J_k{}^T E_k \tag{21}$$

Based on the BP neural network of the LM algorithm, the weight and threshold change are related to the amplitude of the learning rate u_k. The learning rate can be modified during the entire training process. In the early stage of network training, the learning rate is relatively small, which is close to Newton's method. In order to prevent vibrations during the training process and realize the accurate change of the weights in the network, the learning rate increases in the later stage of training and approaches the steepest descent gradient algorithm. Therefore, the LM-BP algorithm combines the advantages of the Newton method and the standard gradient descent method.

4. Simulation results and analysis

This paper uses AnsoftMaxwell software to build a simulation model. As shown in Fig. 3, the tested metal is 1010 steel, and the sensor coil is lifted up to a height of 2mm. In order to enhance the sensitivity of the central area, the adjacent excitation method is used in the experiment. The central area of the sensor is taken as the area of interest, and the area is divided into several grids, and each grid corresponds to a part of the pixels of the image. If the number of grids divided in the region of interest is too much, whether there are cracks in the imaging area will have too little influence on the detection data, resulting in reduced sensitivity. If the number of grids divided in the region of interest is too small, it will cause image reconstruction. The resolution is reduced, it is difficult to determine the details of the smaller defects, and the total number of grids will also affect the image reconstruction time, and finally the region of interest is divided into 100 grids. According to the area of the region of interest, this paper selects a 6-coil sensor structure, each coil has an inner diameter of 10mm and an outer diameter of 12mm. Because this system mainly detects metal defects near the surface, according to the skin effect, the system excitation signal selects a sinusoidal voltage signal of 50kHz.

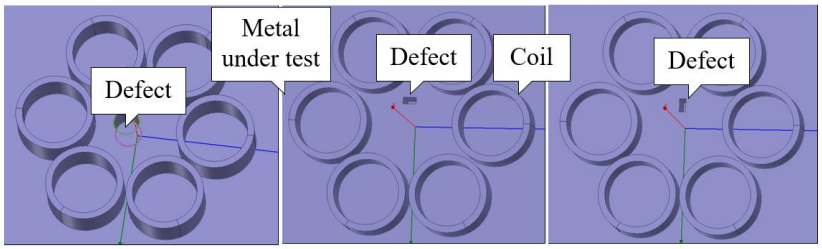

Fig. 3 Software simulation model

This article uses the BP neural network toolbox in Matlab. The main functions include the number of neurons in each layer, the input layer transfer function, the hidden layer transfer function, the hidden layer transfer function, the training function, and the weight learning function. God divides the

network needs a lot of data for training, and divides the collected data into three categories, one is for training the network, the other is for testing the effect of training, and the third is for randomly collected detection data. First, set the input data of the neural network to X, the expected output data is Y, and substitute the data X into the neural network. The actual output data is $\hat{Y}$. By modifying the function intermediate parameters, the error between Y and $\hat{Y}$ is as small as possible. Then, through the verification data to determine the number of network layers and the number of neurons in each layer, etc. In the process of image reconstruction, our goal is to obtain the best verification effect.

In fact, there can be many types of defects in the region of interest. The samples collected in this article contain as many defect distributions as possible. 1000 sets of data are collected for each defect in the region of interest, of which 600 sets are used for training in this situation. The remaining 400 groups are used to verify the effect of the experiment. The distribution of all samples is shown in Fig. 4.

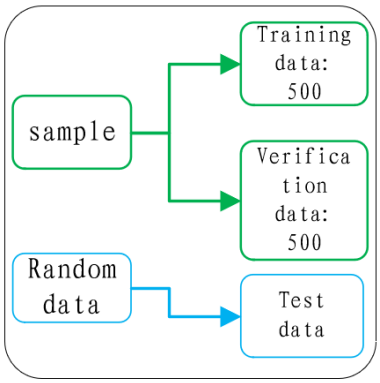

Fig. 4 Simulation data classification

First, the simulation data is normalized, and then trained according to the traditional BP neural network and LM-BP neural network, respectively, and the error curves of the two algorithms after training are obtained, as shown in Fig. 5 and Fig. 6, where Fig. 5 is After the traditional BP neural network is trained, the inspection effect of a certain defect. Fig. 6 shows the inspection effect of a certain defect after the LM-BP neural network training. The green star-shaped curve represents the ideal output, the blue solid curve represents the actual output, and the red circled curve represents the error between the actual output and the expected output.

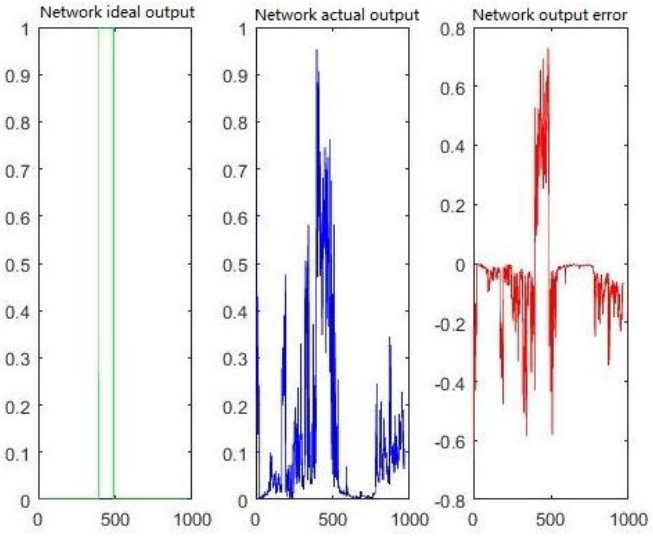

Fig. 5 Traditional BP neural network training results

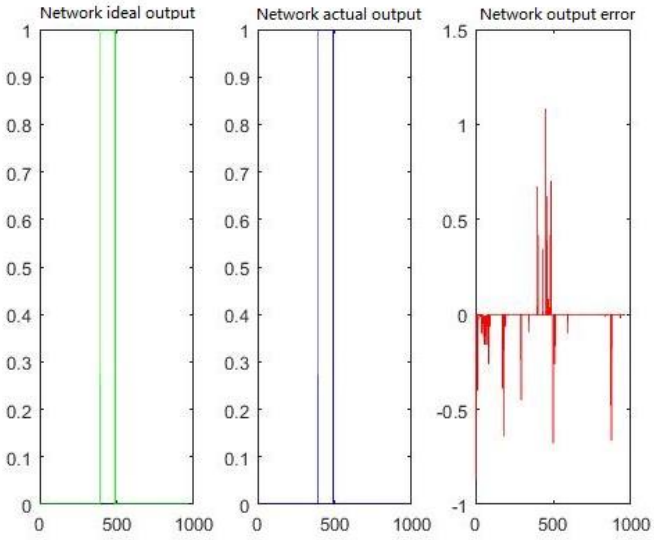

Fig. 6 LM-BP neural network training results

In the experiment, the linear back-projection algorithm and two trained neural networks were used for image reconstruction. The specific results are shown in Fig. 7. It can be seen that the linear back-projection algorithm (LBP) has the worst image reconstruction effect, and the traditional BP neural network algorithm The image reconstruction effect of the linear back projection algorithm (LBP) has been improved to a certain extent, and the LM (Levenberg-Marquardt)-BP neural network algorithm has a greater improvement compared with the traditional BP neural network.

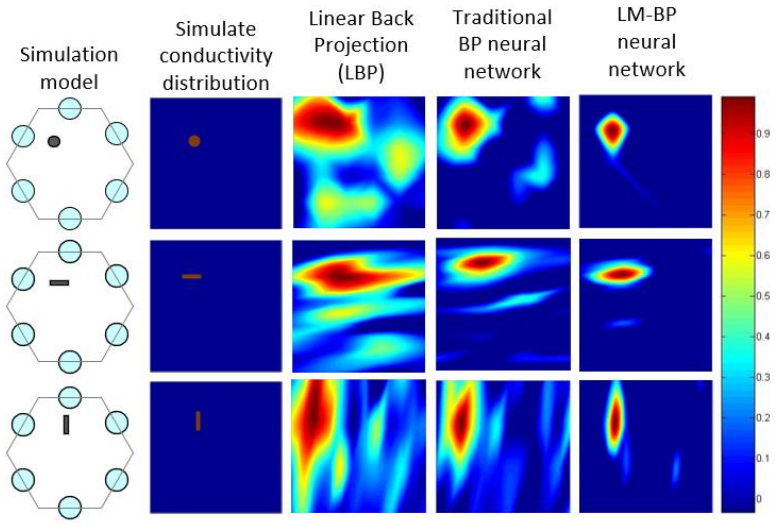

Fig. 7 Image reconstruction effect of different algorithms in simulation

5. Test platform verification

In order to verify the simulation experiment results, a hardware experiment platform was built, as shown in Fig. 8. The specific working principle is as follows: STM32 is used as a controller to control the excitation source to output a sine signal of a certain frequency. After being amplified by the signal conditioning circuit, the DC component is filtered out, and the excitation coil is connected. According to the principle of electromagnetic induction, an induced voltage will be generated on the detection coil. The voltage is related to the surface defects of the tested metal, and then the voltage signal is processed by the signal conditioning circuit and then input to the controller, and finally transmitted to the upper computer through the serial port and image reconstruction is performed.

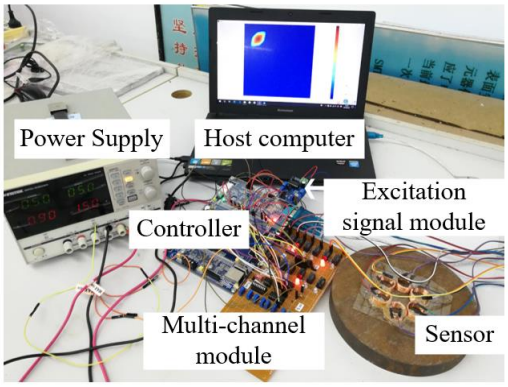

Fig. 8 Experimental EMT flaw detection imaging system

A 6-coil sensor is used in the experiment, as shown in Fig 9, the area of interest is within the red circle and dotted line. In order to improve the sensitivity of the sensor center, the relative excitation method is used.

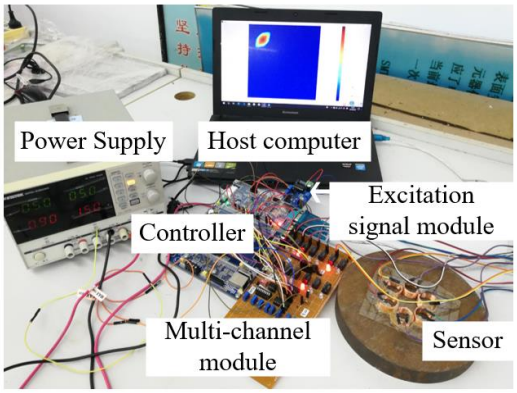

Fig. 9 Six-coil sensor

Use a variety of algorithms to reconstruct the image of the data collected in the experiment. The specific situation is shown in Fig 10. You can see that the image reconstruction effect is based on the linear back projection (LBP) algorithm, the traditional BP neural network algorithm, and the LM-BP neural network. The order of the algorithm is gradually getting better, and the image reconstruction effect of the LM-BP neural network is significantly improved compared with the traditional BP neural network.

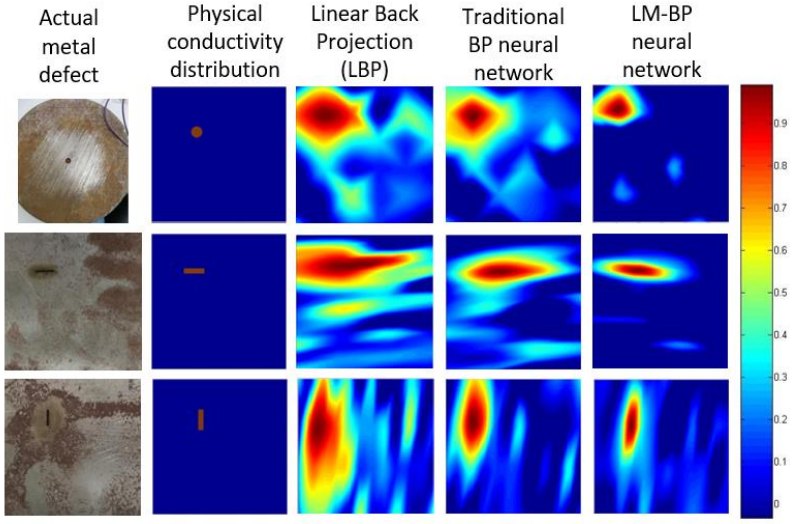

Fig. 10 Image reconstruction effects of different algorithms in the experiment

In order to digitize the image reconstruction effect of the linear back projection algorithm, the traditional BP neural network algorithm and the LM-BP neural network algorithm, the recognition rate is quoted here. In the above image comparison, the 500 groups collected in each defect situation were reconstructed separately, and the recognition rate of each defect situation of different algorithms was obtained, as shown in Fig. 11, and the image of the LM-BP neural network was obtained. The reconstruction recognition rate is higher than the traditional BP neural network and linear back projection algorithm.

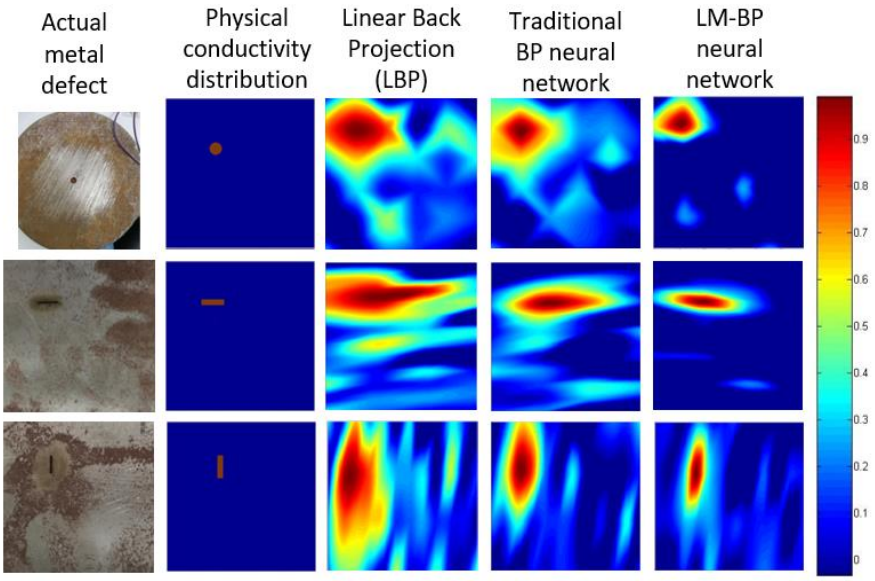

Fig. 11 The recognition rate of different algorithms and different defects in the experiment

6. Test platform verification

First, this article introduces the mathematical model of electromagnetic tomography, and then introduces the shortcomings of the traditional BP neural network algorithm, and then introduces the LM-BP neural network in detail, which theoretically explains that the LM-BP neural network is compared with the traditional BP neural network. The advantages of the network. Finally, simulation and physical experiments were carried out. After comparing the image reconstruction effects of the two algorithms, it was found that the LM-BP neural network algorithm has a greater improvement in the image reconstruction effect than the traditional BP neural network algorithm, which enriches electromagnetic tomography. The feasibility plan.

References

[1] D. Wei Dong, Z.G. Zhou, X.S. Ni. Application of Linear Frequency Modulation Pulse Compression in Air-coupled Ultrasonic Testing[C]. 2010 2nd International Conference on Advanced Computer Control. 2010, pp.53-57.

[2] Y. Zhu, S.C. Wei, Y. Liang, et al. Research Progress of Visual Nondestructive Testing Technology [J]. Material Guide A: Summary, 2017, 31(2) :63-69. (In Chinese).

[3] C. Wang, Y. Zhi, P. Gao. GMR Based Eddy Current System for Defect Detection[C]. The 11 th IEEE International Conference on Electronic Measurement & Instruments. 2013, pp.1052-1056.

[4] Keiji Tsukada, Minoru Hayashi, Yoshihiro Nakamura, et al. Small Eddy Current Testing Sensor Probe Using a Tunneling Magnetoresistance Sensor to Detect Cracks in Steel Structures[J]. IEEE TRANSACTIONS ON MAGNETICS, NOVEMBER 2018, 54(11), DOI: 10.1109/TMAG. 2018. 2845864.

[5] Z.F. Gao. Research on ECT image reconstruction algorithm based on BP neural network [D]. Tianjin: China Civil Aviation University, 2014. (In Chinese).

[6] S.L. Shi. Research on Nonlinear Dynamics Evaluation Model and Application of Mine Safety [D]. Hunan: Central South University, 2000. (In Chinese).

[7] S.K. Li. Fatigue Life Prediction and Application of Hydraulic Support Top Beam Based on LM-BP Neural Network [J]. China Mining, 2019, 28(05): 92-96.

[8] Y.Y. Huang, O. Ou, Y.L. Gan. Combined blind equalization technology based on BP neural network and Newton method [J]. Digital Technology and Application, 2016(06):25. (In Chinese).